Contents lists available at SciOpen

Food Science and Human Wellness

journal homepage: https://www.sciopen.com/journal/2097-0765

China Food Publishing Co.

Cyanidin 3-*O*-*β*-galactoside from black chokeberry ameliorates brain glucose hypometabolism and cognitive impairment in mice through gut microbiota-derived short-chain fatty acids and amino acids

Xiaoyu Liu[a], Zhuoyan Fan[b], Wenjing Jiang[a], Wentao Gao[a], Xinquan Yang[c,*], Jingming Li[a,*]

[a] *College of Food Science and Nutritional Engineering, China Agricultural University, Beijing 100083, China*
[b] *Department of Marine Technology, Rizhao Polytechnic, Rizhao 276826, China*
[c] *Clinical Laboratory Center of Medicine, Zhongshan People's Hospital, Zhongshan 528403, China*

ARTICLE INFO

Article history:
Received 10 October 2024
Received in revised form 10 December 2024
Accepted 27 December 2024

Keywords:
Cyanidin 3-*O*-*β*-galactoside
Cognitive impairment
Streptozotocin
Gut microbiota metabolites
Brain glucose metabolism

ABSTRACT

Neurodegenerative diseases, such as Alzheimer's disease and Parkinson's disease, are associated with cognitive impairment and impaired brain glucose metabolism, posing significant challenges for the public health. We previously demonstrated that cyanidin 3-*O*-*β*-galactoside (Cy3Gal) from black chokeberry alleviated cognitive impairment in aging mice through regulating brain energy metabolism in a direct way. However, the indirect mechanisms in mitigating brain glucose hypometabolism remain underexplored. Here, we utilized a bilaterally intracerebroventricular injection of streptozotocin (ICV/STZ, 3 mg/kg bw)-induced brain glucose hypometabolism model to investigate the effects of Cy3Gal on cognitive impairment alleviation. Our findings revealed that Cy3Gal administration significantly improved memory deficit and cognitive impairment in ICV/STZ-administrated mice. Subsequently, Cy3Gal showed excellent abilities in inhibiting astrocyte overactivation, regulating neurotransmitters metabolism, and promoting synaptic plasticity. Furthermore, Cy3Gal enhanced brain glucose metabolism by improving glycolysis and the TCA cycle. Additionally, Cy3Gal modulated levels of gut microbiota-derived metabolites, including acetate, butyrate, histidine, glutamine, serine, valine and isoleucine, which were closely linked to brain glucose metabolism. The *in vitro* results further demonstrated that these metabolites played an important role in the neuron-astrocyte energy metabolism, which accounted for the alleviation of glucose hypometabolism. Overall, our findings suggest that Cy3Gal mitigates ICV/STZ-induced cognitive impairment by modulating gut microbiota-derived short-chain fatty acids and amino acids, which in turn improves brain glucose metabolism.

1. Introduction

The global rise in aging populations poses a major socioeconomic challenge, particularly due to the increasing incidence and prevalence of neurodegenerative diseases (NDs)[1], such as Alzheimer's disease (AD) and Parkinson's disease (PD), both of which are strongly associated with cognitive dysfunction. Meanwhile, disruptions in brain glucose metabolism are acknowledged as key features of these disorders[2]. Additionally, reduced energy utilization and impaired energy metabolism in neurons can affect the expression of synaptophysin (Syn) and postsynaptic density protein 95 (PSD-95), impairing the ability of neurons to maintain synaptic homeostasis[3]. Streptozotocin (STZ) is a glucosamine-nitrosourea compound isolated from *Streptomyces achromogenes*[4], and the findings demonstrated that a single or double intracerebroventricular injection of STZ could decrease cerebral glucose uptake and produce pathological and behavioral features similar to AD[5-6]. STZ-induced animal model is widely utilized to study the AD-liked symptoms induced by the brain glucose hypometabolism[7].

The human intestine hosts a wide variety of microorganisms from infancy, and the composition of gut microbiota plays a vital role in

* Corresponding authors.
E-mail address: lijingming@cau.edu.cn (J.M. Li); yangxq@gzhu.edu.cn (X.Q. Yang)
Peer review under responsibility of Beijing Academy of Food Sciences.

SciOpen Publishing services by Tsinghua University Press

http://doi.org/10.26599/FSHW.2025.9250496

nutrition, immune responses, and pathological processes[8-9]. Recent research highlights the significant influence of gut microbiota on the development of NDs[10]. Given that dietary components act as substrates for gut microbes, the types and frequency of food intake significantly influence the synthesis of downstream metabolites, contributing to host physiological processes and brain health[11-12]. Among these metabolites, short-chain fatty acids (SCFAs), which are saturated fatty acids with one to six carbon atoms, are particularly important for various metabolic processes[13]. Acetate, propionate, and butyrate are the most abundant SCFAs in the gut, making up over 95% of the total SCFA content[14-15]. Numerous studies have shown a link between lower levels of SCFA-producing bacteria and reduced SCFA concentrations in individuals with mild cognitive impairment and AD[16]. Amino acids (AAs), serving as neurotransmitters, metabolic regulators, and neuromodulators, exert crucial functions in the central nervous system (CNS). The gut microbiota can metabolize and transform numerous AAs, many of which are neurotransmitter participating in brain energy metabolism and impacting brain function[17-18]. In summary, dietary interventions that target the modulation of SCFAs and AAs may offer a promising strategy for preventing NDs and mitigating cognitive decline.

Astrocytes, the most abundant and specialized cell-type in CNS, provide essential metabolic support for neighboring neurons. Notably, astrocytes are highly efficient at absorbing glucose, which they convert primarily into lactate through glycolysis[19]. The lactate shuttle between astrocytes and neurons is essential for maintaining normal brain function. Lactate not only provides energy to neurons, but also mediates long-term memory and increases neuronal excitability[20]. However, during the process of AD and other neurological injuries, astrocytes undergo significant changes in both their structure and function[21], including cell hypertrophy and the upregulation of intermediate filament protein, glial fibrillary acidic protein (GFAP). Recent studies have also highlighted a link between gut microbiota and astrocyte function, showing that changes in gut microbiota composition and metabolites can influence astrocyte proliferation and activity[22]. Therefore, it is possible to maintain neuronal activity by regulating the neuron-astrocyte metabolic coupling.

Our previous study has proved that the dietary intervention of cyanidin 3-*O*-*β*-galactoside (Cy3Gal) combat the decreased brain glucose uptake, contributing to the cognitive improvement. Using PET/CT imaging, we examined glucose metabolism in various regions of the mouse brain, quantifying it with the standard uptake value ratio of ^{18}F-2-fluoro-2-deoxy-*D*-glucose (^{18}F-FDG). Both low and high doses of Cy3Gal reversed the declining trend in glucose uptake[23]. Additionally, we also revealed that Cy3Gal directly regulating the brain glucose metabolism under the challenge high-fat/high-sugar-diet induced glucose disorder, which could be attributed to the improved glucose uptake and metabolism of skeletal muscle and activated mitochondrial respiratory chain complexes[24]. Therefore, given the established link between brain glucose hypometabolism and cognitive impairment, we utilized a bilaterally intracerebroventricular injection of STZ (ICV/STZ)-induced mice model and metabolomic analysis to explore the indirect mechanism by which Cy3Gal alleviates brain glucose hypometabolism and the associated cognitive impairment.

2. Materials and methods

2.1 Chemicals

Cy3Gal (purity ≥ 95%) was purified from black chokeberry (*Aronia melanocarpa* (Michx.) Elliott) in our previous study[25], purity (0.952 g/g) of which is evaluated by HPLC method (Process 1 in the supplementary material and Fig. S1). PSD-95 and interleukin-6 (IL-6) rabbit monoclonal antibody, C3/C3a rabbit polyclonal antibody, bicinchoninic acid (BCA) assay kit, cell counting kit-8 (CCK-8 kit), RIPA lysis buffer was purchased from Beyotime Biotechnology Co., Ltd. (Shanghai, China). GFAP and Syn rabbit polyclonal antibody was purchased from Wuhan Sanying Proteintech Group Inc. (Wuhan, China). All standards (purity ≥ 95%) of glucose-derived intermediates, AAs, SCFAs, neurotransmitters, and STZ were purchased from Sigma Aldrich Co. (St. Louis, MO, USA). All HPLC grade reagents were purchased from Anpel Laboratory Technologies (Shanghai) Inc. (Shanghai, China). All other reagents were of the highest grade commercially available.

2.2 Experimental animal and intervention protocol

The 12–13 weeks old male C57BL/6N (specific pathogen free) mice were obtained from Beijing Vital River Laboratory Animal Technology Co., Ltd. (Beijing, China). All mice were kept in a temperature-controlled ((22 ± 2) °C) animal facility under a 12 h dark-light cycle. Water and food were available ad libitum. After adaption, 40 mice were randomly divided into two groups (n = 10). The model group mice were anesthetized with 5% pentobarbital sodium and fixed on the brain stereotaxic device. After the surface disinfection, an incision was made in the scalp. Subsequently, the needle was inserted vertically 2 mm from the surface of the brain, and STZ was bilaterally ICV injected (3 mg/kg bw, injection volume: 5 μL, injection speed: 0.4 μL/min)[26]. The needle was retained in position for 5 min after the injection. While control (CK) group received bilateral ICV injection of saline. After withdrawing the needle, the incision was locally disinfected and sutured. The injection was repeated at the original position the other day.

Dietary intervention was started 24 h after surgery. The CK and model group mice were orally administrated with 0.2 mL sterile water. While the Cy3Gal-Low and Cy3Gal-High group mice were orally administered with low (25 mg/kg bw) or high (50 mg/kg bw) doses of Cy3Gal, respectively, dissolved in 0.2 mL sterile water. Fasting blood glucose (FBG) was measured every week, and fresh fecal samples were collected after the second week of intervention. All mice were subjected to behavioral tests after 4 weeks of administration. Subsequently, they were anesthetized with 5% pentobarbital sodium, and the serum, brain, and intestinal contents were collected. All experiments were approved by the Animal Ethical and Welfare Committee (No. NKYY-DWLL-2021-001).

2.3 Oral glucose tolerance test (OGTT)

The OGTT was carried out every week according to a previous study[27]. Mice were fasted overnight and then glucose (1.0 g/kg bw) was orally administered. Blood glucose from the tail vein was measured with glucose oxidase method at 0, 30, 60, 90, and 120 min after glucose challenge.

2.4 Y-maze test

After 4-week dietary intervention, the Y-maze test was conducted as previously described with minor modifications[28]. The Y-shaped maze consists of three arms (8 cm × 30 cm × 15 cm, width × length × height) with a 120° angle from each other. Three arms were randomly designated as start arm, food arm and wrong arm. The test includes adaptation, training and testing trials. The camera system recorded the behavior of the animals. The times and total distance of mice entering the food arm within 6 min were recorded as the indexes. Recognition of the food arm from three arms is considered to have the good spatial recognition and memory abilities. All the maze arms were cleaned with 70% ethanol between trials.

2.5 Nissl staining

The collected brains were preserved in 4% paraformaldehyde. Serial coronal sections (25 μm thickness) were prepared using a cryostat (Leica Microsystems, Wetzlar, Germany), which were washed twice for 5 min in 0.01 mol/L PBS and incubated in 1% toluidine blue staining solution for 5–10 min at 20–25 ℃. Then, the sections were rinsed in distilled water, soaked in 95% ethanol for 30 min, and dehydrated in 100% ethanol. After dehydration, the sections were placed in xylene and cover-slipped using resin medium. The number of neurons in the hippocampus and cerebral cortex was quantified using Image-Pro Plus software (Wayne Rasband, NIH, Bethesda, Maryland, USA).

2.6 Immunofluorescence staining

Fixed brain sections were rehydrated and subjected to antigen retrieval in citric acid antigen repair buffer (pH 6.0) for 10 min at 95–100 ℃. Tissues were then blocked with bovine serum albumin (BSA) for 30 min, then incubated in primary antibody (anti-Syn, 1:500; anti-PSD-95, 1:200; anti-C3, 1:200; anti-GAFP, 1:200, 4 ℃) and florescent secondary antibody (goat anti-rabbit, 1:400, 2 h at 25 ℃). After antibody incubation, nuclear staining was performed using 4′,6-diamidino-2-phenylindole (DAPI). The sections were visualized using fluorescent microscope (Olympus, Tokyo, Japan). Images were analyzed with ImageJ software.

2.7 Western blot analysis

The frozen brains were homogenized in RIPA lysis buffer and centrifuged at 12 000 × *g* for 15 min. Protein concentrations were determined using a BCA assay kit. The protein samples were separated by SDS-PAGE, transferred to the polyvinylidene fluoride (PVDF) membrane, and blocked with 5% skim milk for 2 h. The PVDF membrane was then incubated with specific primary antibodies (anti-PSD-95, 1:1 000; anti-Syn, 1:1 000; anti-IL-6, 1:1 000; anti-GFAP, 1:1 000) at 4 ℃. Horseradish peroxidase binding secondary antibody was incubated with the PVDF membrane. The proteins were visualized by chemiluminescence reagents and analyzed using the gel recording system (GelDoc-It 310 imaging system).

2.8 Metabolomic analysis

2.8.1 Determination of brain glucose metabolism intermediates

Intermediates of glucose metabolism in brain samples were extracted and determined using ultra-high performance liquid chromatography-mass spectrometry (UPLC-MS) method, as performed in Process 2 in the supplementary material. All the intermediates were identified and quantified according to the standards (Table S1).

2.8.2 AAs content measurement

AAs in brain, serum, colonic contents, and cecal contents were extracted and determined using UPLC-MS methods[29], as performed in Process 3 in the supplementary material. All the AAs were identified and quantified according to the standards (Tables S2–S3).

2.8.3 SCFAs content measurement

SCFAs in brain, serum, colonic content and cecal content were extracted (Process 4 in the supplementary material) and detected by gas chromatography. Bruker Scion 456-GC coupled with Agilent DB-FFAP column (30 m × 0.25 mm, 0.25 μm, J&W Scientific, Folsom, CA, USA) was employed. Helium was used as carrier gas and at a flow rate of 1.0 mL/min. Injection was made in the split mode at a ratio of 10:1 and the injection volume were 1 μL. The oven temperature was held at 80 ℃ for 2 min, raised to 180 ℃ at a rate of 10 ℃/min and held at 180 ℃ for 2 min, then raised to 230 ℃ at a rate of 3 ℃/min and held at 230 ℃ for 5 min. Flame ionization detector was employed for detection at 240 ℃. All the SCFAs were identified and quantified according to the standards (Table S4).

2.8.4 Neurotransmitters content measurement

Neurotransmitters in the brain were extracted and determined using UPLC-MS method[29], as performed in Process 5 in the supplementary material. All the neurotransmitters were identified and quantified according to the standards (Table S5).

2.9 Cell culture and treatment

HT22 cells and GL261 cells (BeNa Culture Collection, Beijing, China) were cultured in DMEM (containing 25 mmol/L glucose) and DMEM/F-12 (containing 17.5 mmol/L glucose) with 10% fetal bovine serum and 1% penicillin-streptomycin, respectively. Briefly, cells were seeded into 96-well plates (100 μL/well) and treated with different concentrations of glutamine, histidine, isoleucine, serine, valine, sodium acetate, and sodium butyrate. After incubation for 24 and 48 h, the cells were washed twice with PBS, then 100 μL medium and 10 μL CCK-8 reagent was added for an additional 1 h. Finally, the cell viability was determined according to instructions.

Subsequently, we focused on the effects of Mixture I (acetate, butyrate, histidine, glutamine, and serine) and Mixture II (isoleucine and valine) on the neuron-astrocyte metabolic coupling. Briefly, HT22 and GL261 cells were seeded into the upper and lower chambers of a Transwell system until 80% confluence, respectively. Afterwards,

the original medium was removed and the cells were starved with EBSS for 2 h. Furthermore, the treatment of each group was described in Table S6. Following 48-h incubation, the medium was collected to detect the concentrations of glucose and lactate according to the assay kits (Nanjing Jiancheng Bioengineering Research Institute, Nanjing, China), and the HT22 cells were collected to detect the ATP content. GL261 cells were collected to determine the expression of GFAP by Western blot, following the protocol described in Section 2.7.

2.10 Statistical analysis

Data are presented as mean ± standard deviation. The test data were processed by one-way ANOVA using the SPSS version 20.0 software package. Multiple comparisons of the data were performed via Tukey's test, which was used to compute significant differences at $P < 0.05$, $P < 0.01$ and $P < 0.001$.

3. Results

3.1 Cy3Gal alleviated memory deficit and cognitive impairment

The 12–13 weeks old mice received oral administration of a vehicle solution and Cy3Gal for 4 weeks, followed by behavioral tests and biochemical analysis (Fig. 1A). To assess the potential of Cy3Gal in improving cognitive function, the Y-maze test was performed on ICV/STZ-administered mice. The number of entering the correct arm ($P < 0.05$, Fig. 1B), the total time to explore in the correct arm ($P < 0.001$, Fig. 1C) and the total moving distance in the correct arm ($P < 0.001$, Fig. 1D) in model group were significantly reduced compared with CK group. Notably, the administration of Cy3Gal at both low and high doses markedly ameliorated the cognitive deficits ($P < 0.05$, $P < 0.01$, $P < 0.001$, Fig. 1), illustrating the mitigating effects of Cy3Gal on cognitive impairment in ICV/STZ-administrated mice.

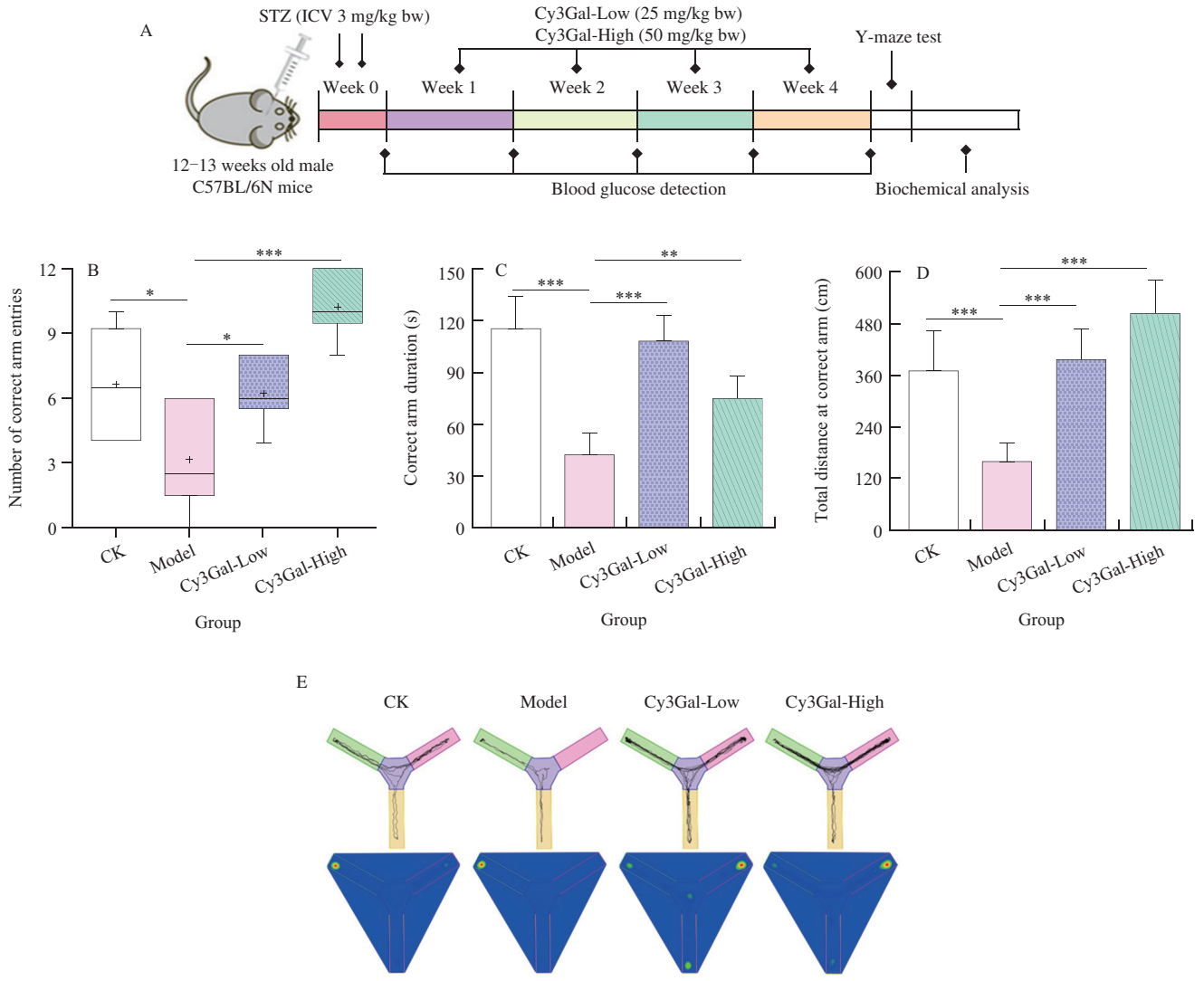

Fig. 1 Cy3Gal alleviated cognitive impairment in STZ-administrated mice ($n = 6$). (A) Experimental workflow of animal treatments. (B) The number of entering the correct arm of mice in Y-maze. (C) The duration time in the correct arm. (D) The total moving distance of mice in the correct arm. (E) Representative action tracks (upper panel) and heat maps of action track (lower panel) of mice among different groups. *$P < 0.05$, **$P < 0.01$, ***$P < 0.001$.

3.2 Cy3Gal improved glycolysis and TCA cycle metabolism in brain

Within confines of the CNS, STZ can impede the process of glucose uptake and metabolism in neuronal cells, leading to compromised energy and glucose utilization in the brain, potentially culminating in cognitive decline[30]. Firstly, we diligently tracked the FBG levels of mice both before and after a 4-week period following the ICV/STZ. The results revealed that both STZ injection and Cy3Gal intervention had no significant impact on the FBG levels ($P > 0.05$, Fig. S2), which was consistent with the previous research[31]. Furthermore, levels of glycolysis intermediates in ICV/STZ-administrated mice decreased compared with CK mice (Fig. 2A), including fructose 1,6-bisphosphate ($P < 0.01$), glyceric acid 3-phosphate ($P < 0.01$), glyceric acid 2-phosphate ($P < 0.01$) and pyruvate ($P < 0.001$). However, Cy3Gal treatment markedly elevated the concentrations of these intermediates. In addition, Cy3Gal-Low and Cy3Gal-High intervention significantly increased lactate levels compared to model group ($P < 0.01$, Fig. 2A), implying that Cy3Gal effectively enhanced glycolysis metabolism in the brain.

Regarding the TCA cycle, notable reductions were observed in various intermediates compared to the CK group, including acetyl-CoA, citrate, isocitrate, α-ketoglutarate, succinyl-CoA, fumarate and oxaloacetate, levels of which were decreased by 34.19%, 25.38%, 17.36%, 31.09%, 33.59%, 16.20%, and 21.38%, respectively (Figs. 2B–H). While Cy3Gal intervention reversed the decline of these intermediates except for α-ketoglutarate. Additionally, the results highlighted that Cy3Gal-Low and Cy3Gal-High treatment significantly enhanced the NAD^+/NADH ratio (fold change (FC) of Cy3Gal-Low and model (FC_{Low}) = 1.68, $P < 0.001$; FC of Cy3Gal-High and model (FC_{High}) = 1.80, $P < 0.001$, Fig. 2L) and reduced AMP/ATP ratio (FC_{Low} = 0.71, $P < 0.001$; FC_{High} = 0.83, $P < 0.01$, Fig. 2M). Therefore, these findings suggested that Cy3Gal could improve brain energy metabolism in ICV/STZ-administrated mice by enhancing glycolysis and modulating TCA cycle pathway.

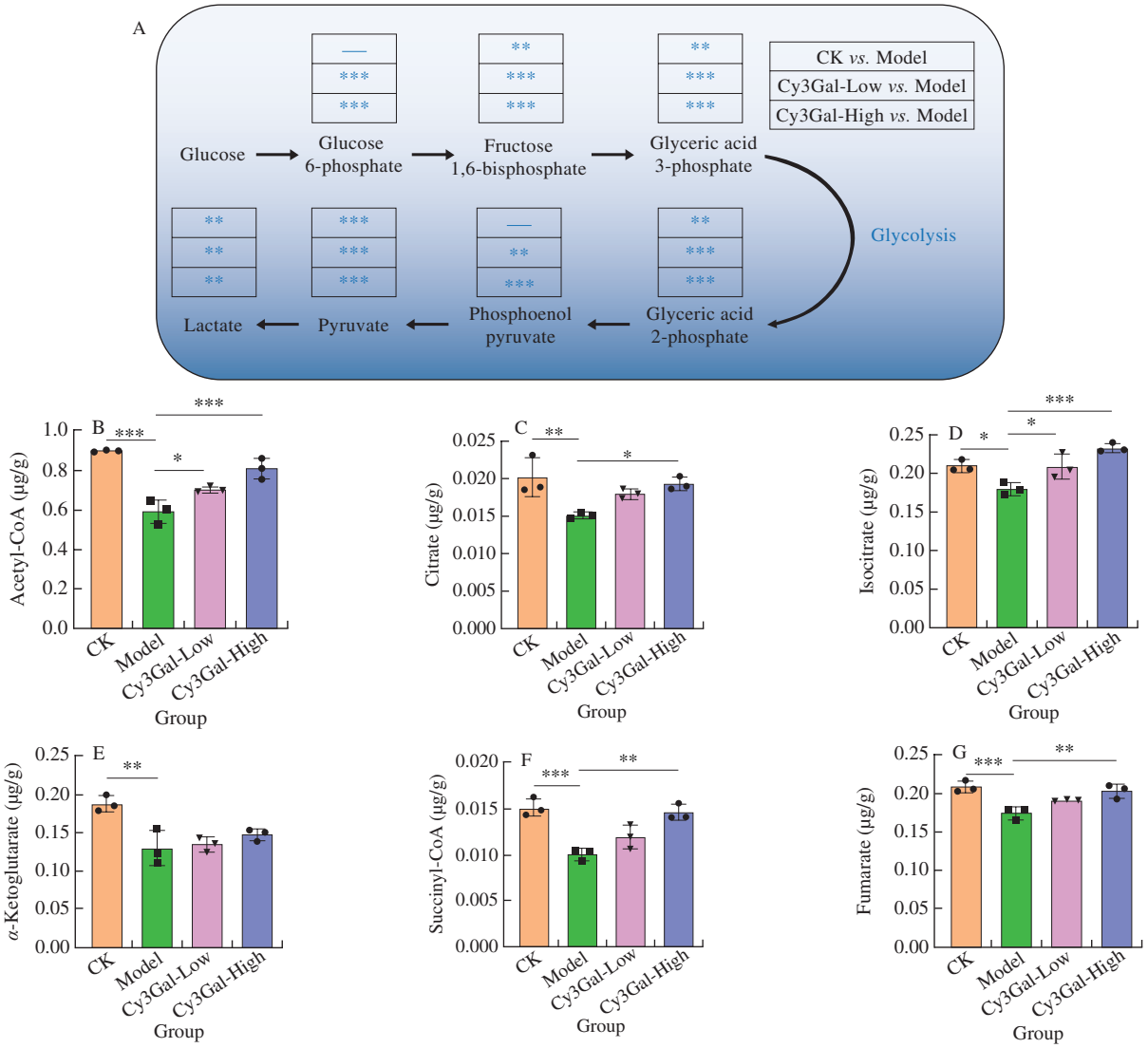

Fig. 2 Cy3Gal enhanced glycolysis and TCA cycle metabolism of brain in STZ-administrated mice ($n = 3$). (A) Cy3Gal increased glycolysis intermediates accumulation to augment TCA cycle metabolism in brain of STZ-administrated mice. (B-K) Levels of TCA circle-related intermediates in brain tissues among different groups. (L) NAD^+/NADH ratio among different groups. (M) AMP/ATP ratio among different groups. *$P < 0.05$, **$P < 0.01$, ***$P < 0.001$.

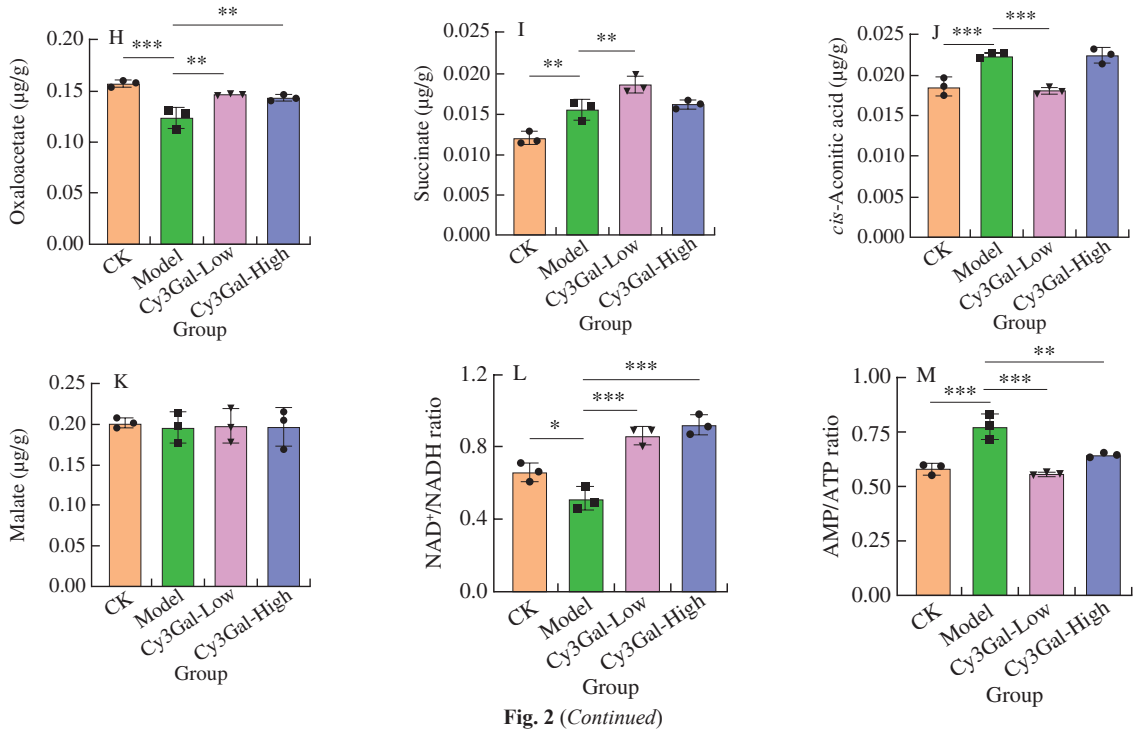

Fig. 2 (*Continued*)

3.3 Effect of Cy3Gal intervention on the correlations between gut microbiota metabolites and glucose metabolism intermediates

Convincing evidences support the hypothesis that SCFAs and AAs produced by the gut microbiota could act as essential role in regulating energy metabolism. We analyzed the levels of SCFAs and AAs in the colonic contents, cecal contents, brain, and serum of mice (Tables S7–S11). The results demonstrated that acetate and butyrate levels significantly decreased in the model group ($P < 0.001$, Fig. 3A), which were reversed by Cy3Gal intervention. In contrast, STZ induction and Cy3Gal treatment exhibit inconsistent effects on the levels of different AAs (Fig. 3B). Interestingly, the levels of acetate, butyrate, glutamate, glycine, histidine, glutamine, tryptophan, and serine demonstrated a primarily positive correlation with the concentrations of key glucose metabolism intermediates (Fig. 3C). Conversely, the concentrations of alanine, isoleucine, methionine, tyrosine, and valine were found to exhibit a negative correlation. These metabolites could potentially act as crucial mediators involved in the regulation of brain glucose metabolism in Cy3Gal-treated mice.

Furthermore, a pronounced relationship was evidenced through a comparative analysis of the alterations in levels of SCFAs and AAs across different sections. Interestingly, the results indicated that the levels of glutamine, histidine, isoleucine, glycine, serine, and valine in serum and brain were positively correlated ($P < 0.001$, Fig. 3D). Additionally, levels of glutamine and serine in the cecal and colonic contents exhibited a significant positive correlation with those in the serum ($P < 0.001$). Dietary supplementation of serine was found to ameliorate dyslipidemia and attenuate diabetes-induced peripheral neuropathy in mice[32]. The concentration of histidine in colonic contents and that of isoleucine in cecal contents both showed positive correlations with those in serum ($P < 0.001$). Restricting intake of isoleucine or valine had the potential to reshape hepatic lipid metabolism, enhance hepatic insulin sensitivity, and boost energy consumption[33]. Valine levels in cecal and colonic contents were found to be negatively and positively correlated with those in serum ($P < 0.001$, Fig. 3E), respectively. Collectively, these results indicated that there was a strong relationship between the levels of acetate, butyrate, glutamine, histidine, serine, isoleucine, and valine and brain glucose metabolism.

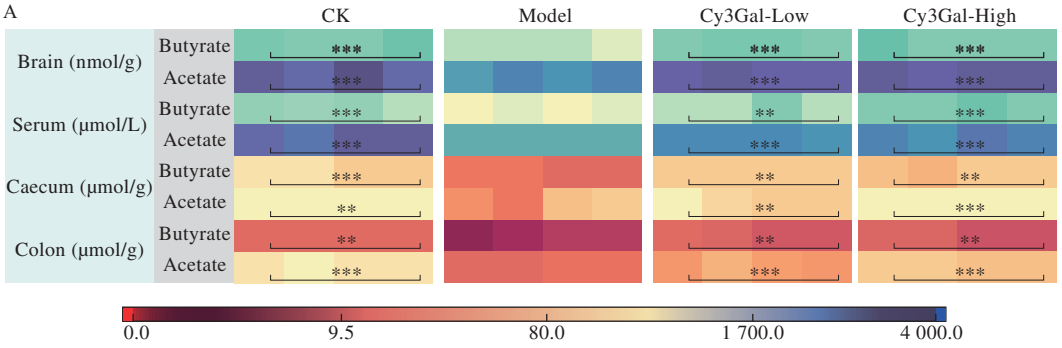

Fig. 3 Effect of Cy3Gal treatment on the content and correlation of SCFAs and AAs ($n = 4$). (A) Levels of acetate and butyrate in brain, serum, cecal contents, and colonic contents of mice. (B) Levels of AAs in brain, serum, cecal contents, and colonic contents of mice. (C) Correlation analysis between SCFAs, AAs and key intermediates of glucose metabolism in the brain. (D) Correlation analysis of AAs between brain and serum. (E) Correlation analysis of AAs between serum and cecal/colonic contents. *$P < 0.05$, **$P < 0.01$, ***$P < 0.001$.

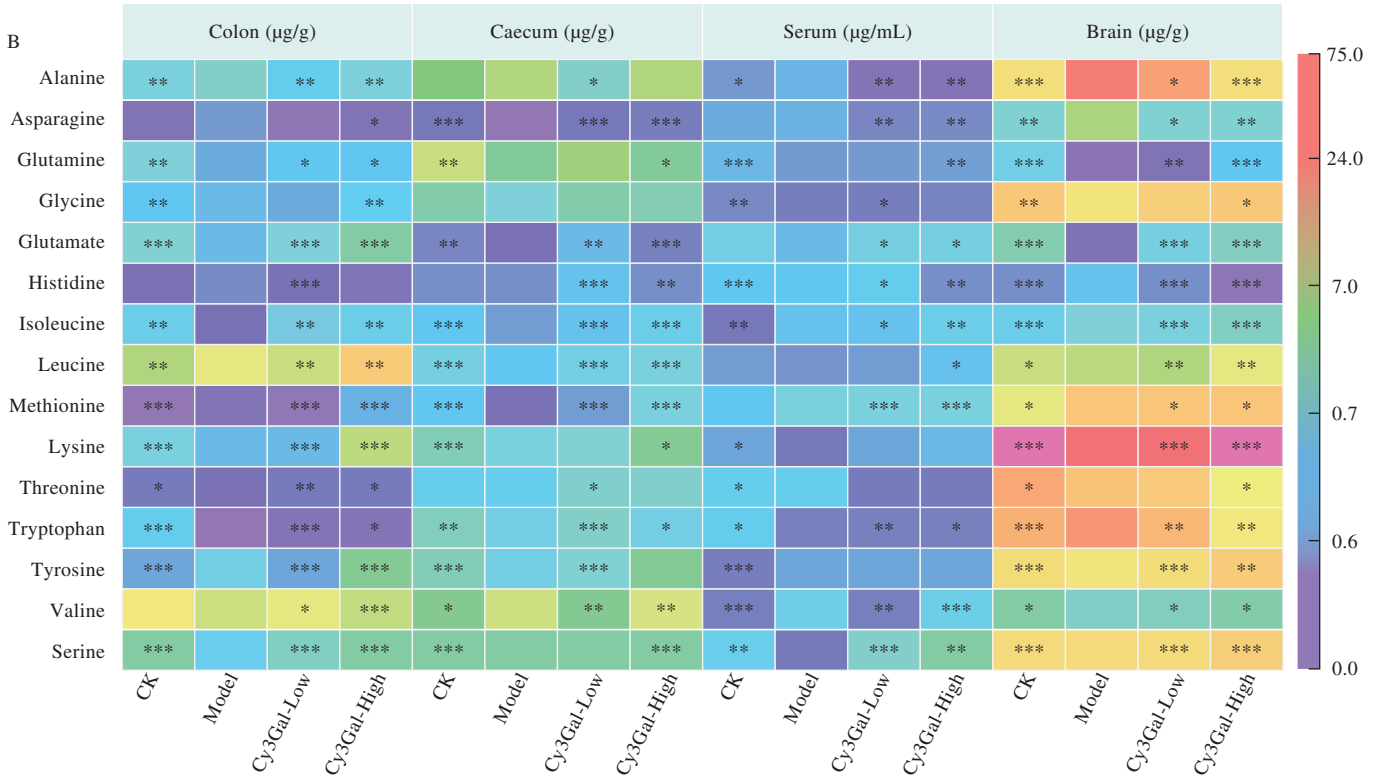

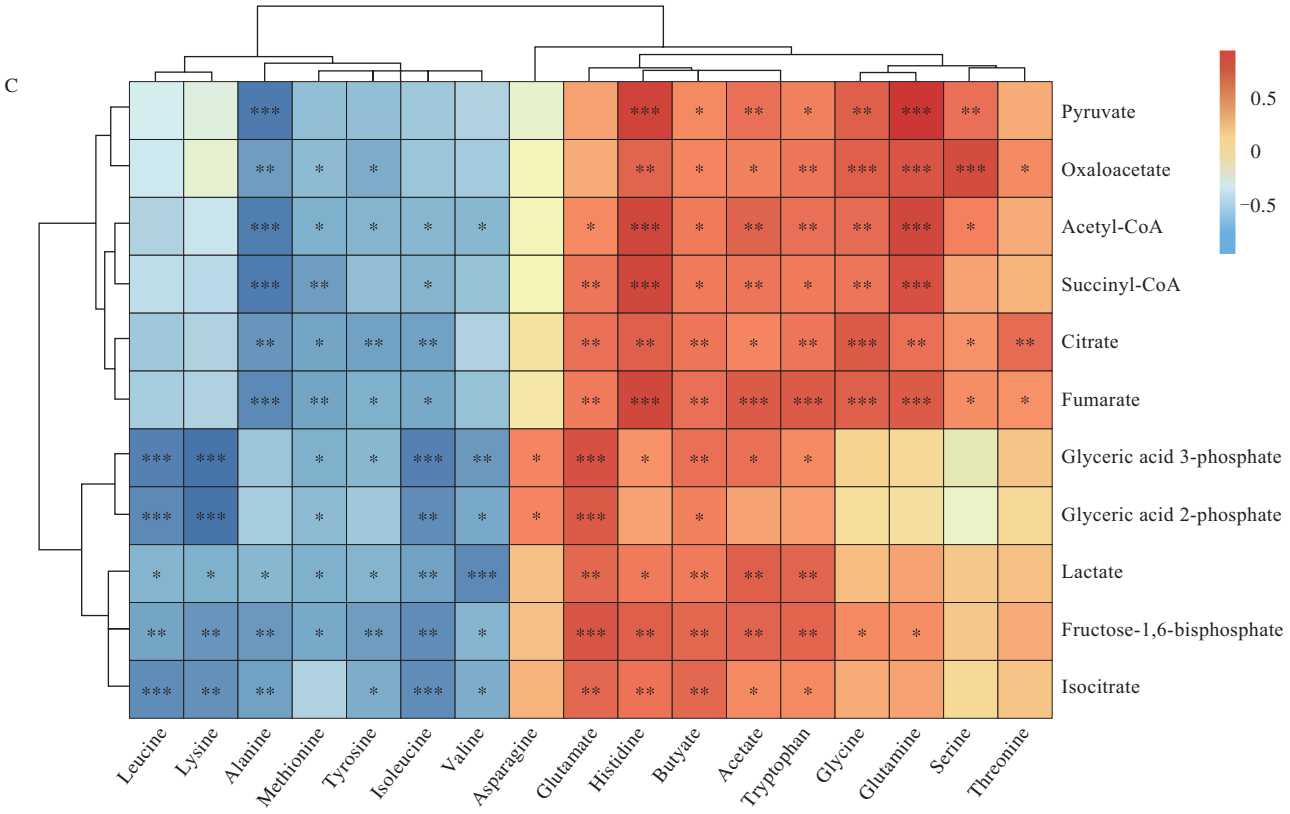

Fig. 3 (*Continued*)

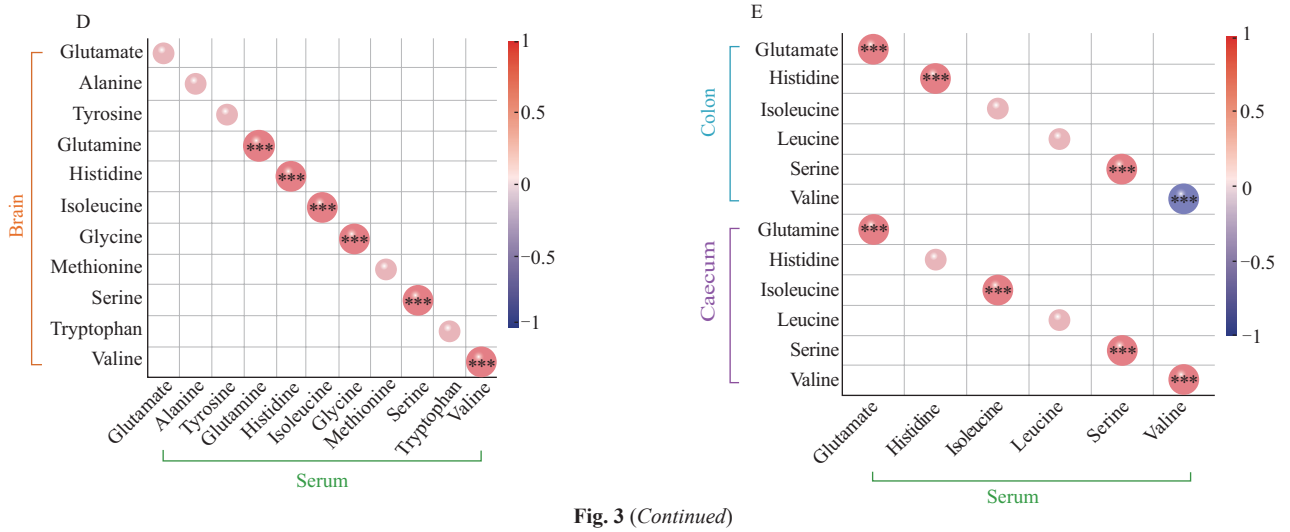

Fig. 3 (*Continued*)

3.4 Cy3Gal inhibited the hyperproliferation and hyperactivation of astrocytes

Astrocytes, classified as innate immune cells, play a pivotal role in the CNS as they synthesize and release nerve growth factors and neurotransmitters, which enhance neuronal survival and inhibit neuronal apoptosis[34-35]. We employed complement C3 and GFAP as biomarkers to evaluate the activation state of astrocytes in the hippocampus. The results showed that C3/GFAP-positive cells were abundant in CA1, CA2, CA3 and DG regions of the hippocampus in model group, while their quantity in CK and Cy3Gal-treated mice exhibited a significant decrease (Fig. 4A). Furthermore, both Cy3Gal-Low and Cy3Gal-High treatment significantly decreased the immunofluorescence intensity of C3 ($P < 0.05$, $P < 0.001$, Fig. 4B) and GFAP ($P < 0.05$, $P < 0.01$, Fig. 4B) in astrocytes. Additionally, we observed a notable increase in GFAP expression within the cerebral cortex of the model group ($P < 0.05$, Fig. 4D), a trend that was effectively reversed by Cy3Gal-High treatment ($P < 0.05$, Figs. 4C–D), while Cy3Gal-Low had no significant effect ($P > 0.05$, Fig. 4D). Subsequently, we observed a significant increase in the expression of IL-6 in the

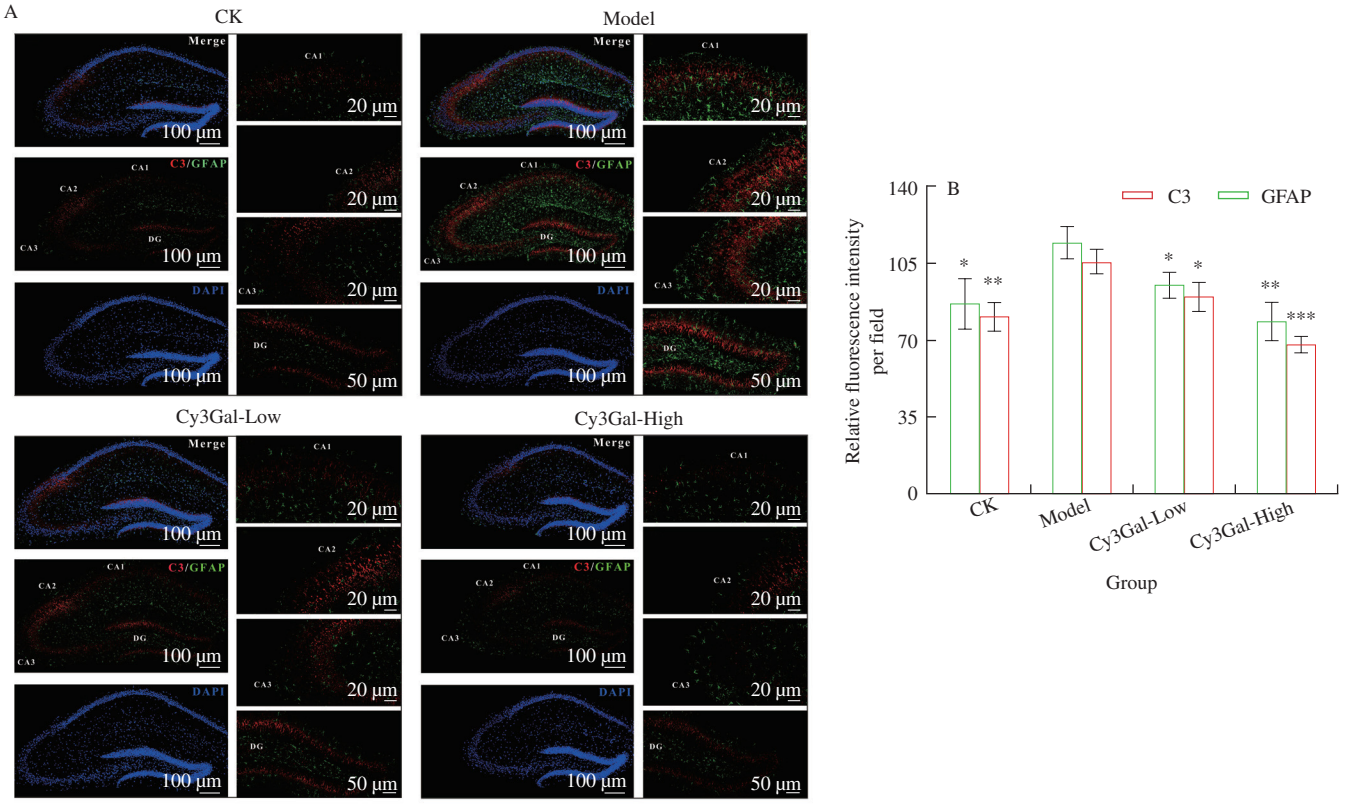

Fig. 4 Cy3Gal inhibited hyperproliferation and hyperactivation of astrocytes in STZ-administrated mice ($n = 3$). (A) Representative immunofluorescence staining sections of C3 and GFAP in the mice hippocampus from different groups. (B) Quantification of positive area based on immunofluorescence staining sections. (C) Representative Western blots of GAFP and IL-6. (D) Relative optical density of GAFP and IL-6. *$P < 0.05$, **$P < 0.01$, ***$P < 0.001$, compared with the model group.

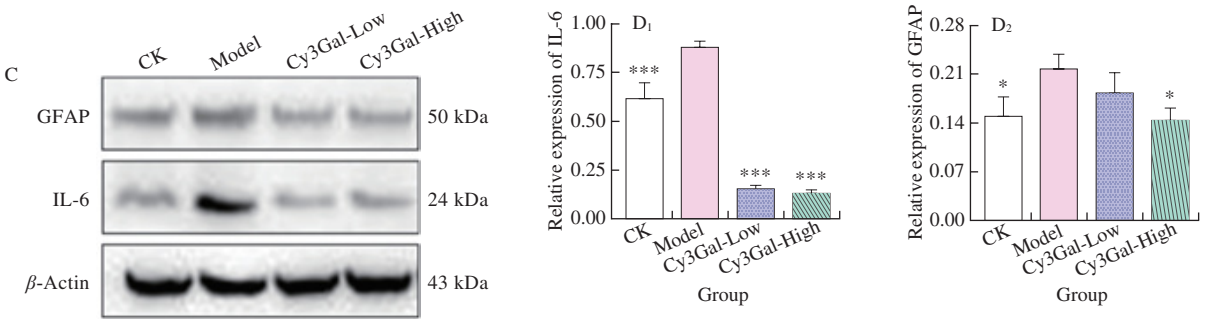

Fig. 4 (*Continued*)

model group ($P < 0.001$), which was markedly attenuated by both Cy3Gal-Low and Cy3Gal-High treatments ($P < 0.001$, Fig. 4D). These results suggested that Cy3Gal possessed the capability to suppress the exaggerated activation and inflammatory reactions of astrocytes in the hippocampus and cerebral cortex of mice under conditions of compromised brain energy metabolism, which play a crucial role in maintaining the normal physiological activities of neurons.

3.5 Cy3Gal exerted neuronal protection through enhancing synaptic plasticity and regulating the metabolism of neurotransmitters

Considering memory and cognitive impairment are closely related to neuronal damage in hippocampus and cerebral cortex, pathological examination of hippocampal neurons was performed. Nissl staining results illustrated the orderly and compact arrangement of hippocampal neurons in CK mice, characterized by distinct nuclei and prominent Nissl bodies within the cytoplasm, as highlighted by red arrows in Fig. 5A. However, neurons in CA1, CA2, and CA3 regions exhibited sparse distribution and cytoplasmic atrophy in the model group. Concurrently, the majority of neurons displayed Nissl body depletion, accompanied by a significant increase in neuronal apoptosis and loss. In contrast, Cy3Gal intervention ameliorated neuronal degeneration and injury, characterized by distinct round or oval nuclei and numerous Nissl bodies. Most of the energy acquired by neurons is used to generate neuronal action potentials and transmit information between synapses. The immunofluorescence staining results indicated a reduction in synaptic density within the hippocampus of model mice, with a more pronounced loss of local synapses compared to the CK group (Figs. 5B–C). However, Cy3Gal exerted a potent reversal of these alterations. Synaptic density was notably augmented within the hippocampus, accompanied by a significant elevation in the fluorescence intensity of Syn and PSD-95 in Cy3Gal-Low group ($P < 0.01$, Fig. 5D). While high dose of Cy3Gal demonstrated a better effect on Syn expression of the hippocampus ($P < 0.001$, Fig. 5D). Meanwhile, the Western blotting results showed that Cy3Gal-Low increased the expression of both Syn and PSD-95 ($P < 0.01$, Figs. 5E–F), while Cy3Gal-High only increased the Syn expression ($P < 0.05$, Fig. 5F), indicating the potential of Cy3Gal to enhance synaptic plasticity of neurons.

Regulation of neurotransmitter homeostasis is a pivotal function of astrocytes within the CNS[36]. The results showed that eight neurotransmitters were significantly decreased compared to CK group except for 5-hydroxy-*L*-tryptophan (5-HTP), including acetylcholine, kynurenic acid, norepinephrine, tryptamine,

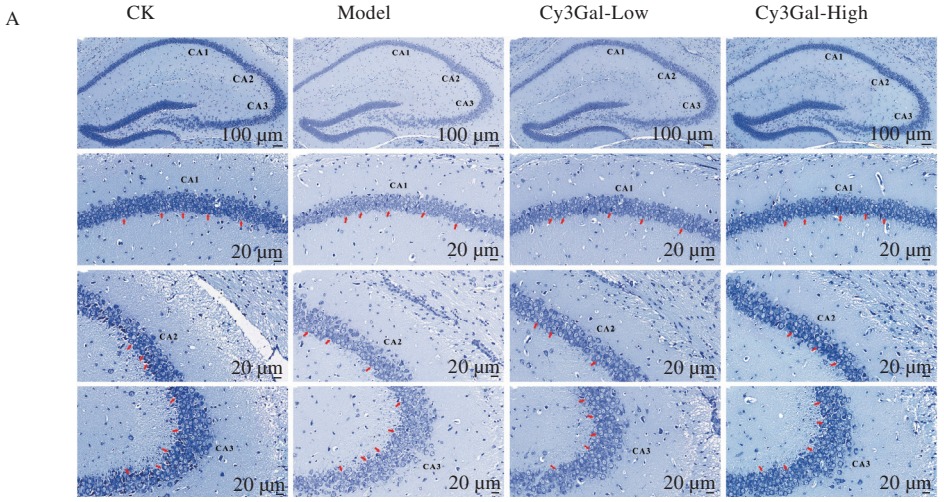

Fig. 5 Cy3Gal protected synapses from damage in STZ-administrated mice ($n = 3$). (A) Representative Nissl staining images of the CA1, CA2 and CA3 regions in the mice hippocampus from different groups. (B) Representative immunofluorescence staining sections of PSD-95 (green) in the brain. (C) Representative immunofluorescence staining sections of Syn (red) in the brain. (D) Quantification of positive area based on immunofluorescence staining sections. (E) Representative Western blots of Syn and PSD-95. (F) Relative optical density of Syn and PSD-95. *$P < 0.05$, **$P < 0.01$, ***$P < 0.001$, compared with the model group.

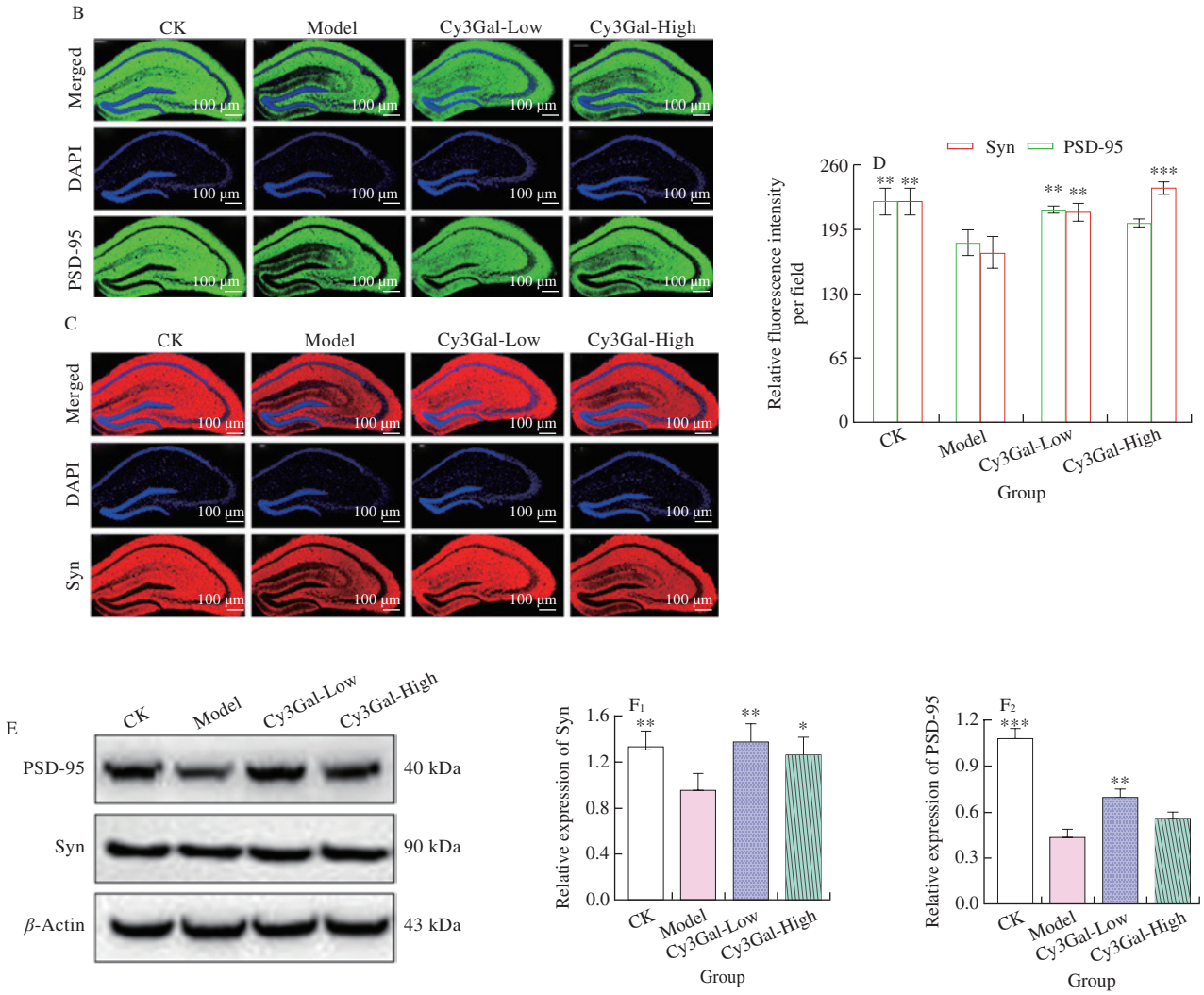

Fig. 5 (*Continued*)

dopamine, GABA, 5-hydroxyindoleacetic acid (5-HIAA), and 5-hydroxytryptamine (5-HT). While Cy3Gal treatment reversed the changes. The levels of acetylcholine ($P < 0.01$, $P < 0.001$), dopamine ($P < 0.001$, $P < 0.01$), norepinephrine ($P < 0.01$, $P < 0.001$), tryptamine ($P < 0.01$) and GABA ($P < 0.01$, $P < 0.001$) were significantly modulated by Cy3Gal-Low and Cy3Gal-High treatment (Fig. 6A), while Cy3Gal-High intervention also significantly increased the levels of 5-HTP, 5-HT and 5-HIAA ($P < 0.001$, $P < 0.01$, Fig. 6A). These results demonstrated that Cy3Gal intervention helped regulate neurotransmitter synthesis and metabolism in the brain of the ICV/STZ-administrated mice. Furthermore, we observed positive correlations between glutamine and neurotransmitters such as glycine, 5-HIAA, 5-HT, dopamine, acetylcholine, and GABA (Fig. 6B). This suggested that glutamine may enhance the synthesis of these neurotransmitters, thereby improving neuronal communication and cognitive functions. Similarly, histidine and serine showed strong positive correlations with major neurotransmitters (Fig. 6B), indicating their supportive roles in neurotransmitter synthesis and regulation. Conversely, negative correlations between isoleucine and neurotransmitters such as glutamate and tryptamine (Fig. 6B) suggest that elevated levels of isoleucine may inhibit neurotransmitter synthesis or activity, potentially impairing neuronal function. Valine also shows similar negative correlations (Fig. 6B), highlighting its potential detrimental impact on neurotransmitter levels. These results are consistent with the association between AAs and brain glucose metabolism intermediates. However, the levels of alanine, methionine, tyrosine, glycine, glutamate, and tryptophan in the mouse brain were also influenced by Cy3Gal intervention. Our results revealed significant enhancement in synaptic plasticity and direct/indirect regulation of neurotransmitters after Cy3Gal treatment.

3.6 Effects of the five AAs and SCFAs on neuron-astrocyte metabolic coupling

We employed an HT22-GL261 co-culture system (Fig. 7A) to verify the effects of brain glucose metabolism-associated AAs and SCFAs on neuron-astrocyte metabolic coupling, along with the involvement of astrocytes in the regulation of neuronal energy metabolism[37]. Analysis of cell viability suggested that 8 mmol/L glutamine, 0.5 mmol/L

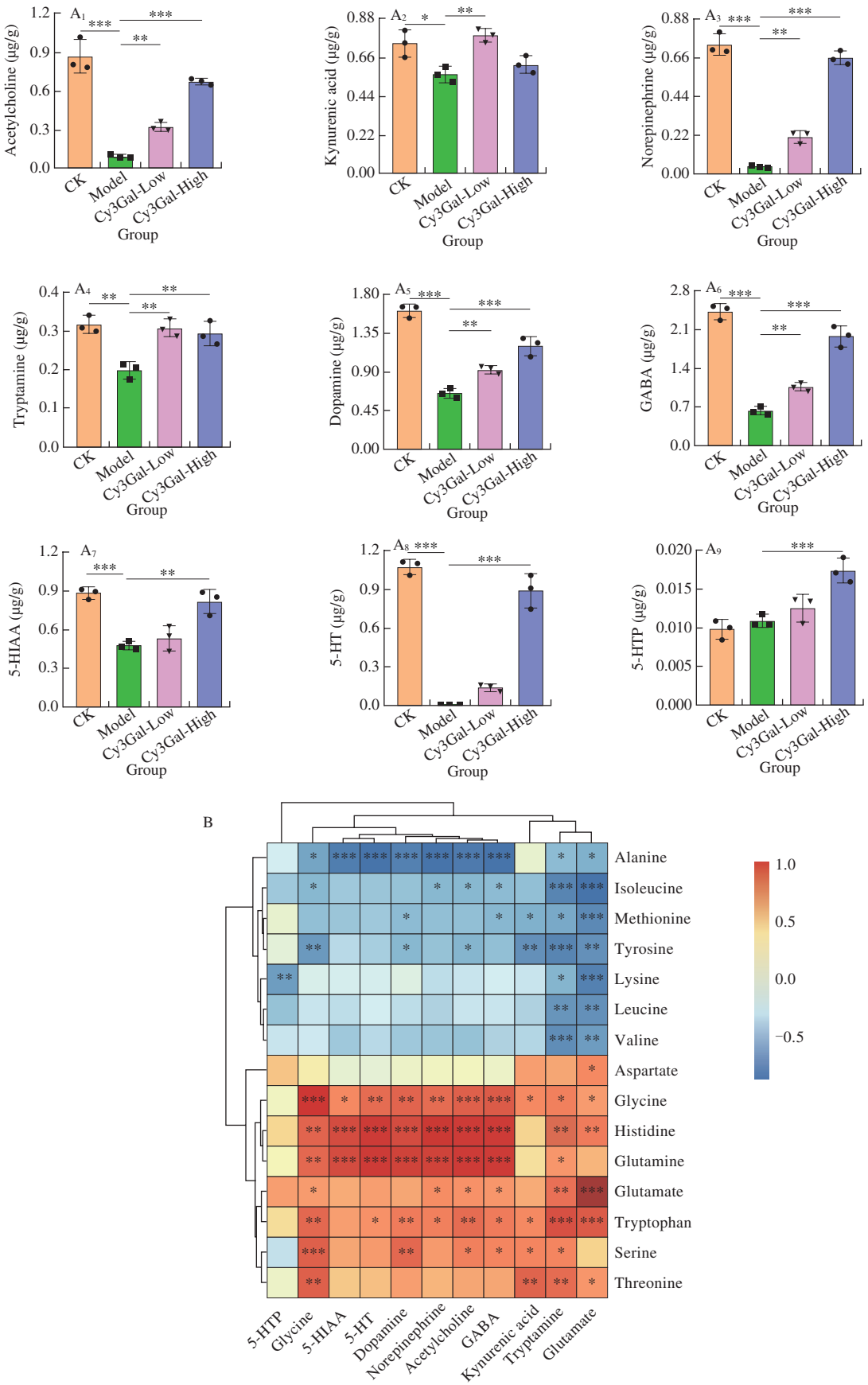

Fig. 6 Effect of Cy3Gal intervention on the alternation of neurotransmitters in mice brain ($n = 3$). (A) Levels of the neurotransmitters in mice brain among different groups. (B) Correlation analysis between AAs and neurotransmitters in the brain. *$P < 0.05$, **$P < 0.01$, ***$P < 0.001$.

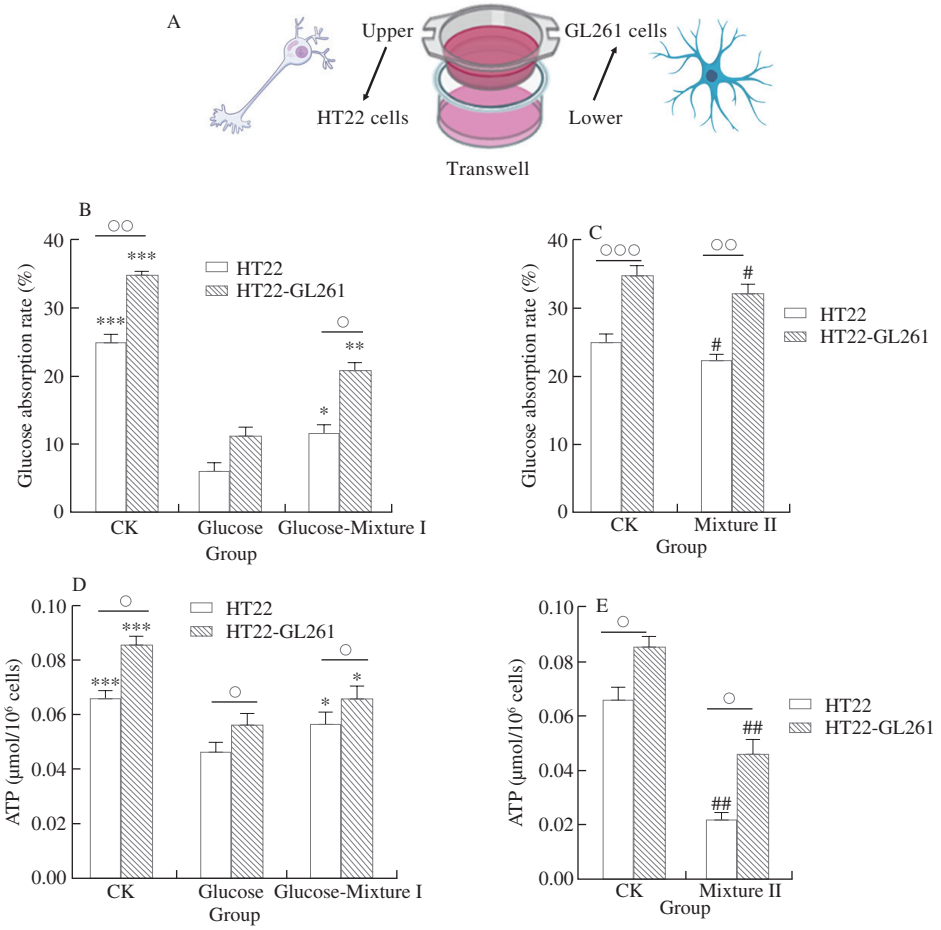

Fig. 7 Effects of brain glucose metabolism-associated AAs and SCFAs on neuron-astrocyte metabolic coupling ($n = 3$). (A) Cell experiment performance. (B, D) Effects of high-glucose environment and Mixture I treatment on the glucose consumption rate and ATP production of HT22 cells. (C, E) Effects of Mixture II treatment on the glucose consumption rate and ATP production of HT22 cells. *$P < 0.05$, **$P < 0.01$, ***$P < 0.001$, compared with the Glucose group; $^{\#}P < 0.05$, $^{\#\#}P < 0.01$, compared with the CK group; °$P < 0.05$, °°$P < 0.01$, °°°$P < 0.001$.

histidine, 0.1 mmol/L serine, 0.1 mmol/L valine, 0.5 mmol/L isoleucine, 0.5 mmol/L butyrate, and 15 mmol/L acetate were chosen for the subsequent experiments (Figs. S3−S4). Furthermore, we employed a high-glucose (50 mmol/L glucose) culture environment to mimic the situation in the brain of STZ-induced brain glucose hypometabolism model. The results indicated that the viability of HT22 and GL261 cells was 85.25% and 88.35% ($P < 0.01$, $P < 0.05$, Fig. S5), respectively, which was suitable for the experiment. Additionally, Mixture I significantly enhanced the viability of HT22 cells ($P < 0.001$) and had no significant effect on GL261 cells ($P > 0.05$). Mixture II had no significant effect on the viability of either HT22 or GL261 cells ($P > 0.05$).

Initially, we examined the effects of Mixture I and Mixture II on the glucose absorption in HT22 cells. In the HT22 cells individual culture group, the glucose absorption rate was significantly reduced in the high-glucose environment ($P < 0.001$), which was promoted by Mixture I treatment ($P < 0.05$, Fig. 7B). The same results were observed in the co-culture system. Additionally, the glucose absorption of co-culture group was significantly promoted compared to individual culture in a normal environment ($P < 0.01$). Furthermore, high-glucose treatment significantly decreased the ATP production of HT22 cells in both individual culture and co-culture group ($P < 0.001$), while Mixture I reversed the changes ($P < 0.05$). Afterwards, ATP production in HT22 cells was fostered by co-culturing with GL261 cells under both normal and high-glucose conditions ($P < 0.05$, Fig. 7C). Overall, acetate, butyrate, histidine, glutamine, and serine were capable of enhancing glucose absorption and augmenting energy production to protect the HT22 cells from damage of high-glucose. Meanwhile, GL261 cells can participate in the regulation of energy metabolism. Subsequently, we observed that Mixture II notably reduced the glucose absorption rate of HT22 cells in both individual culture and co-culture group ($P < 0.05$, Fig. 7D). Additionally, Mixture II also reduced the level of ATP in both individual culture and co-culture group ($P < 0.01$, Fig. 7E). Meanwhile, ATP production in HT22 cells was significantly enhanced when co-cultured with GL261 cells ($P < 0.05$). In summary, isoleucine and valine had a negative effect on glucose uptake and metabolism in HT22 cells, which was alleviated by GL261 cells.

Astrocytes are considered as the “glycolytic” cell, lactate released by which is the main energy source of neurons and is necessary to maintain neuronal activity[38]. We observed a significant reduction of lactate released by GL261 cells in high-glucose environment compared to normal environment ($P < 0.001$, Fig. 8A), while Mixture I treatment reversed the situation ($P < 0.001$). However, lactate content of HT22 cells in normal and Mixture I group was lower than that in high-glucose environment ($P < 0.05$, Fig. 8A), implying that lactate

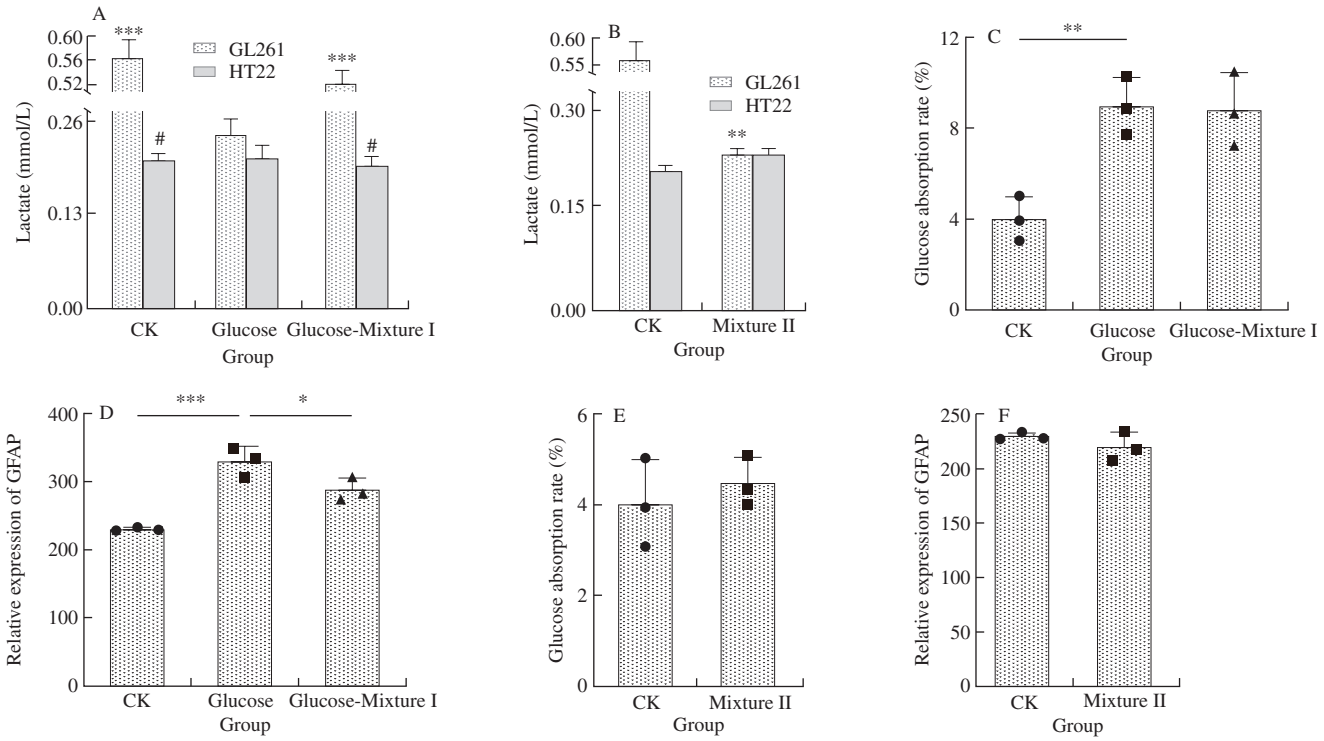

Fig. 8 Effects of brain glucose metabolism-associated AAs and SCFAs on energy metabolism and activation of GL261 cells (n = 3). (A) Effects of high-glucose environment and Mixture I treatment on the lactate level of GL261 and HT22 cells. (B) Effects of Mixture II treatment on the lactate level of GL261 and HT22 cells. (C-D) Effects of high-glucose environment and Mixture I treatment on the glucose consumption rate and GFAP expression of GL261 cells. (E-F) Effects of Mixture II treatment on the glucose consumption rate and GFAP expression of GL261 cells. *P < 0.05, **P < 0.01, ***P < 0.001;$^{\#}P$ < 0.05, compared with the Glucose group.

uptake by HT22 cells from GL261 cells was impeded under high-glucose conditions. Furthermore, Mixture II significantly decreased the lactate content of GL261 cells (P < 0.01, Fig. 8B), while Mixture II treatment had no significant effect on the lactate content in HT22 cells (P > 0.05, Fig. 8B). Furthermore, we found that glucose absorption rate of GL261 cells was significantly enhanced under high-glucose stimulation (P < 0.01, Fig. 8C). However, Mixture I treatment did not significantly alter it, as well as Mixture II (P > 0.05, Figs. 8C and E). However, astrocytes experience glucose metabolism dysregulation in a high-glucose environment. Despite increased glucose uptake, abnormal glycogen storage occurs, leading to a reduction in the metabolic efficiency and capacity of astrocytes[39]. It is consistent with the decrease in lactate levels secreted by GL261 cells in high-glucose environment.

Changes in astrocyte activity and function affect their energy supply and lactate release. We observed that expression of GAFP was significantly increased after high-glucose stimulation (P < 0.001), and Mixture I treatment reversed the situation (P < 0.05, Fig. 8D). Moreover, we observed that Mixture II had no significant effect on activation of GL261 cell (P > 0.05, Fig. 8F). Acetate, butyrate, histidine, glutamine, and serine are capable of mitigating the deleterious effects of high-glucose environment on neuronal cells and enhance the glucose metabolism capacity. Conversely, isoleucine and valine exhibit a negative regulatory effect on the glucose metabolism of neuronal cells.

4. Discussions

The decline in brain glucose metabolism is a key factor in the onset and progression of AD. With the help of positron emission tomography (PET) with ^{18}F-FDG, a proof-of-concept study revealed that glucose hypometabolism was detected in the brain of ICV/STZ-administrated rats[40]. In our study, after ICV/STZ treatment, the mice brain exhibited signs of energetic stress, likely leading to an enhanced glycolytic pathway as a compensatory mechanism to mitigate the energy crisis (Fig. 5A)[37]. Specifically, Cy3Gal ameliorated disruptions in brain glucose metabolism by reversing ICV/STZ-induced reductions in key glycolysis and TCA cycle intermediates. This was evidenced by a notable increase in levels of lactate, pyruvate, acetyl-CoA, isocitrate, and oxaloacetate (Fig. 2). Meanwhile, the elevated NAD^+/NADH ratio suggested that Cy3Gal enhanced glucose metabolism in brain[41]. These changes in turn regulated the concentrations of ATP and NADH and improved the energy state in the mice brain. Consequently, we observed that Cy3Gal exerted profound effects in alleviating neuron loss and improve cognitive impairment in STZ-induced mice (Figs. 1, 4–5). Moreover, the balance between NAD^+ and NADH can regulates activities of various dehydrogenases, and directly or indirectly affect metabolic pathways, cell aging, and other key cellular functions[42]. The Cy3Gal-mediated evaluation of NAD^+/NADH ratio in brain could be attributed to its outstanding antioxidant properties and its capacity to augment antioxidant activities in neurons, thereby reinforcing neuroprotective effects. Anthocyanins benefit from colonic microbiota-mediated

degradation[43], which improves their bioavailability and potentially contributes to their antioxidant activity.

Additionally, alternations of gut microbiota metabolites in Cy3Gal-treated mice significantly influenced the brain glucose metabolism (Fig. 2). Previous research has demonstrated that anthocyanins, including Cy3Gal, have low bioavailability, with only small amounts entering systemic circulation. Instead, a substantial portion of unabsorbed anthocyanins accumulates in the large intestine and are metabolized by the gut microbiota to generate SCFAs and other metabolites, contributing to the nutritional effects[44-45]. Notably, Firmicutes and Bacteroidetes have been strongly linked to metabolic disorders. Firmicutes contain a greater number of carbohydrate-metabolizing enzymes, which play a critical role in energy metabolism in the body[46]. A previous study showed that tea polyphenols effectively reduced the Firmicutes/Bacteroidetes (F/B) ratio, significantly increased SCFAs production, and reduced intestinal permeability, thus maintaining the integrity of the intestinal barrier[47]. Moreover, Tian et al.[48] demonstrated that ferulic acid (FA) significantly promoted SCFA-producing bacteria in the intestine, leading to increased SCFA levels and enhanced expression of SCFA receptors. Additionally, FA reduced intestinal permeability, substantially strengthened the intestinal barrier, and alleviated gut inflammation. These findings provide valuable insights into the potential mechanism by which Cy3Gal regulates the gut microbiota and intestinal barrier. After Cy3Gal intervention, levels of acetate and butyrate exhibited a consistent increase in brain, serum, colonic and cecal contents compared to model group. Particularly, acetate can be integrated into the TCA cycle by combining with oxaloacetate to form citrate, generating energy in the form of ATP[49]. Similarly, butyrate can be converted to acetyl-CoA and enter the TCA cycle[50]. Furthermore, glutamine can be converted into glutamate, and subsequently into α-ketoglutarate, directly feeding into the TCA cycle[51]. Serine can be converted into pyruvate, a key end-product of glycolysis and an entry molecule for the TCA cycle[52]. This multifaceted metabolic enhancement suggests that Cy3Gal ameliorates the ICV/STZ-induced metabolic dysregulation, highlighting its potential to mitigate the brain glucose hypometabolism. Moreover, reductions of brain aerobic glycolysis are often observed at the early stages of AD[53]. The *in vitro* results demonstrated that Mixture I (acetate, butyrate, histidine, glutamine, and serine) treatment enhanced the glycolytic activity and suppressed the activation of astrocytes in high-glucose environment, while Mixture II (isoleucine and valine) only inhibited the production of lactate (Fig. 8). Furthermore, Mixture I promoted the glucose absorption and ATP production, offering protection to neuron cells in high-glucose environment. However, isoleucine and valine showed an inhibitory effect on the glucose uptake and metabolism of HT22 cells (Fig. 7). Additionally, astrocytes play a key regulatory role in the neuronal energy metabolism[39], and the brain glucose metabolism-associated SCFAs and AAs can influence neuronal energy metabolism through metabolic coupling between neurons and astrocytes.

Meanwhile, the previous study had indicated that ICV/STZ-administrated mice exhibited AD-like cognitive impairments, including the reduced spontaneous movement, exploratory behavior, and the impaired learning and memory ability[26]. Consistent with these findings, we observed decreased cognitive performance after ICV/STZ administration. However, Cy3Gal reversed the situation, as indicated by increases in the number, total distance, total distance entering the correct arm (Fig. 1), which could be attributed to the inhibition of astrocyte overactivation and promotion of synaptic plasticity. Astrocytes are critical regulators of neuronal metabolism and neurovascular coupling, helping to supply energy for neuronal activity[54]. However, ICV/STZ induces astrocyte overactivation and increases the release of inflammatory factors in the hippocampus[26]. Astrocyte overactivation often occur early in AD, even before Aβ deposition, with reactive astrocyte hyperplasia marked by increased GFAP expression[55]. GFAP, a marker of astrocyte activation, is related to the formation of the blood-brain barrier[56]. Our findings revealed the profound impact of Cy3Gal on anti-neuroinflammation and astrocyte physiology. Cy3Gal significantly reduced the overactivation of astrocytes, as evidenced by decreased expression of GFAP and C3, along with a notable reduction of IL-6 (Figs. 4B, D). Furthermore, Synaptic plasticity, essential for learning and memory abilities, is often disrupted by chronic neuroinflammation, leading to the loss of synapse-related proteins and neuronal injury[57]. However, ICV/STZ induced an imbalanced expression of synaptic plasticity related proteins in the hippocampus of mice. Furthermore, Cy3Gal treatment increased the number of neurons in the hippocampus (Fig. 5A), enhanced the expression of Syn and PSD-95 (Figs. 5B−F), and regulated the levels of glutamate and GABA, which are the main excitatory neurotransmitter and inhibitory neurotransmitter in the brain[58-59]. Additionally, the age-related glucose metabolism pattern has been suggested as a potential marker for brain aging in cognitively normal elderly individuals[60]. In previous studies, we demonstrated that Cy3Gal treatment improved brain glucose metabolism and preserved neuronal and synaptic health in a 4-week-old mouse model[24]. The results provide a valuable foundation and complement to the current research. These findings indicated the protective effects of Cy3Gal on the nervous system in the brain. These results underscore the protective effects of Cy3Gal on the CNS, particularly through balancing astrocyte activity and regulating neurotransmitter levels. This highlights the potential of Cy3Gal as a nutritional intervention to mitigate synaptic dysfunction and cognitive impairment.

5. Conclusion

In summary, we revealed that Cy3Gal could enhanced the brain glucose metabolism indirectly by modulating the gut microbiota-derived SCFAs and AAs in the ICV/STZ-administrated mice, at *in vivo* and *in vitro* level, which ensured the brain energy supply and eventually alleviated the cognitive impairment. These findings not only revealed the nutritional benefits of dietary anthocyanins (Cy3Gal) in NDs but also underscore the importance of a systemic perspective in understanding and treating cognitive impairments induced by brain glucose hypometabolism.

Declaration of competing interest

The authors declare no competing financial interest.

Acknowledgement

This work was supported by the National Natural Science Foundation of China (32172210) and the Shandong Provincial Natural Science Foundation (ZR2025QC295).

Appendix A. Supplementary data

Supplementary data associated with this article can be found, in the online version, at http://doi.org/10.26599/FSHW.2025.9250496.

References

[1] F. Nazam, S. Shaikh, N. Nazam, et al., Mechanistic insights into the pathogenesis of neurodegenerative diseases: towards the development of effective therapy, Mol. Cell. Biochem. 476 (2021) 2739-2752. https://doi.org/10.1007/s11010-021-04120-6.

[2] S. Dewanjee, P. Chakraborty, H. Bhattacharya, et al., Altered glucose metabolism in Alzheimer's disease: role of mitochondrial dysfunction and oxidative stress, Free Radic. Biol. Med. 193 (2022) 134-157. https://doi.org/10.1016/j.freeradbiomed.2022.09.032.

[3] S.C. Cunnane, A. Courchesne-Loyer, C. Vandenberghe, et al., Can ketones help rescue brain fuel supply in later life? Implications for cognitive health during aging and the treatment of Alzheimer's disease, Front Mol. Neurosci. 9 (2016) 53. https://doi.org/10.3389/fnmol.2016.00053.

[4] J. Weller, A. Budson, Current understanding of Alzheimer's disease diagnosis and treatment, F1000Research 7 (2018) 1161. https://doi.org/10.12688/f1000research.14506.1.

[5] P. Grieb, Intracerebroventricular streptozotocin injections as a model of Alzheimer's disease: in search of a relevant mechanism, Mol. Neurobiol. 53 (2016) 1741-1752. https://doi.org/10.1007/s12035-015-9132-3.

[6] T.O. Santos, C.H. Mazucanti, G.F. Xavier, et al., Early and late neurodegeneration and memory disruption after intracerebroventricular streptozotocin, Physiol. Behav. 107 (2012) 401-413. https://doi.org/10.1016/j.physbeh.2012.06.019.

[7] L. Zhang, C. Chen, M.S. Mak, et al., Advance of sporadic Alzheimer's disease animal models, Med. Res. Rev. 40 (2020) 431-458. https://doi.org/10.1002/med.21624.

[8] M. Blaut, T. Clavel, Metabolic diversity of the intestinal microbiota: implications for health and disease, J. Nutr. 137 (2007) 751S-755S. https://doi.org/10.1093/jn/137.3.751S.

[9] H.R. Wachsmuth, S.N. Weninger, F.A. Duca, Role of the gut-brain axis in energy and glucose metabolism, Exp. Mol. Med. 54 (2022) 377-392. https://doi.org/10.1038/s12276-021-00677-w.

[10] B. Hu, Y. Shi, C. Lu, et al., Raspberry polyphenols alleviate neurodegenerative diseases: through gut microbiota and ROS signals, Food Funct. 14 (2023) 7760-7779. https://doi.org/10.1039/d3fo01835k.

[11] H.B. Dodiya, H.L. Lutz, I.Q. Weigle, et al., Gut microbiota-driven brain Aβ amyloidosis in mice requires microglia, J. Exp. Med. 219 (2022) e20200895. https://doi.org/10.1084/jem.20200895.

[12] T.R. Sampson, J.W. Debelius, T. Thron, et al., Gut microbiota regulate motor deficits and neuroinflammation in a model of Parkinson's disease, Cell 167 (2016) 1469-1480.e12. https://doi.org/10.1016/j.cell.2016.11.018.

[13] K.A. Krautkramer, J. Fan, F. Backhed, Gut microbial metabolites as multi-kingdom intermediates, Nat. Rev. Microbiol. 19 (2021) 77-94. https://doi.org/10.1038/s41579-020-0438-4.

[14] D.J. Morrison, T. Preston, Formation of short chain fatty acids by the gut microbiota and their impact on human metabolism, Gut Microbes 7 (2016) 189-200. https://doi.org/10.1080/19490976.2015.1134082.

[15] R. Mirzaei, B. Bouzari, S.R. Hosseini-Fard, et al., Role of microbiota-derived short-chain fatty acids in nervous system disorders, Biomed. Pharmacother. 139 (2021) 111661. https://doi.org/10.1016/j.biopha.2021.111661.

[16] T. Doifode, V.V. Giridharan, J.S. Generoso, et al., The impact of the microbiota-gut-brain axis on Alzheimer's disease pathophysiology, Pharmacol. Res. 164 (2021) 105314. https://doi.org/10.1016/j.phrs.2020.105314.

[17] B.D. Needham, R. Kaddurah-Daouk, S.K. Mazmanian, Gut microbial molecules in behavioural and neurodegenerative conditions, Nat. Rev. Neurosci. 21 (2020) 717-731. https://doi.org/10.1038/s41583-020-00381-0.

[18] J.A. Pedroso, T.T. Zampieri, J.J. Donato, Reviewing the effects of *L*-leucine supplementation in the regulation of food intake, energy balance, and glucose homeostasis, Nutrients 7 (2015) 3914-3937. https://doi.org/10.3390/nu7053914.

[19] Y. Itoh, T. Esaki, K. Shimoji, et al., Dichloroacetate effects on glucose and lactate oxidation by neurons and astroglia *in vitro* and on glucose utilization by brain *in vivo*, Proc. Natl. Acad. Sci. U.S.A. 100 (2003) 4879-4884. https://doi.org/10.1073/pnas.0831078100.

[20] P.J. Magistretti, I. Allaman, Lactate in the brain: from metabolic end-product to signalling molecule, Nat. Rev. Neurosci. 19 (2018) 235-249. https://doi.org/10.1038/nrn.2018.19.

[21] Z. Chen, Z. Yuan, S. Yang, et al., Brain energy metabolism: astrocytes in neurodegenerative diseases, CNS Neurosci. Ther. 29 (2023) 24-36. https://doi.org/10.1111/cns.13982.

[22] L. Xu, X. Zeng, Y. Liu, et al., Inhibitory effect of *Dendrobium officinale* polysaccharide on oxidative damage of glial cells in aging mice by regulating gut microbiota, Int. J. Biol. Macromol. 247 (2023) 125787. https://doi.org/10.1016/j.ijbiomac.2023.125787.

[23] Z. Fan, H. Wen, X. Zhang, et al., Cyanidin 3-*O*-*β*-galactoside alleviated cognitive impairment in mice by regulating brain energy metabolism during aging, J. Agric. Food Chem. 70 (2022) 1111-1121. https://doi.org/10.1021/acs.jafc.1c06240.

[24] Z. Fan, X. Liu, W. Gao, et al., Cyanidin 3-*O*-*β*-galactoside from black chokeberry exerts neuroprotective effects in mice fed with high-fat/high-sugar diet through regulating glucose metabolism, Food Sci. Hum. Wellness 14(11) (2025) 9250275. https://doi.org/10.26599/FSHW.2024.9250275.

[25] H. Wen, H. Cui, H. Tian, et al., Isolation of neuroprotective anthocyanins from black chokeberry (*Aronia melanocarpa*) against amyloid-β-induced cognitive impairment, Foods 10 (2020) 63. https://doi.org/10.3390/foods10010063.

[26] M. Fan, S. Liu, H.M. Sun, et al., Bilateral intracerebroventricular injection of streptozotocin induces AD-like behavioral impairments and neuropathological features in mice: involved with the fundamental role of neuroinflammation, Biomed. Pharmacother. 153 (2022) 113375. https://doi.org/10.1016/j.biopha.2022.113375.

[27] S. Suzuki, S. Aoe, High *β*-glucan barley supplementation improves glucose tolerance by increasing GLP-1 secretion in diet-induced obesity mice, Nutrients 13 (2021) 527. https://doi.org/10.3390/nu13020527.

[28] M. van de Wouw, A.M. Walsh, F. Crispie, et al., Distinct actions of the fermented beverage kefir on host behaviour, immunity and microbiome gut-brain modules in the mouse, Microbiome 8 (2020) 67. https://doi.org/10.1186/s40168-020-00846-5.

[29] F. Zhang, Y. Wan, T. Zuo, et al., Prolonged impairment of short-chain fatty acid and *L*-isoleucine biosynthesis in gut microbiome in patients with COVID-19, Gastroenterology 162 (2022) 548-561.e4. https://doi.org/10.1053/j.gastro.2021.10.013.

[30] Y. Zhang, R. Ding, S. Wang, et al., Effect of intraperitoneal or intracerebroventricular injection of streptozotocin on learning and memory in mice, Exp. Ther. Med. 16 (2018) 2375-2380. https://doi.org/10.3892/etm.2018.6487.

[31] K. Bloch, I. Gil-Ad, A. Vanichkin, et al., Intracranial transplantation of pancreatic islets attenuates cognitive and peripheral metabolic dysfunctions in a rat model of sporadic Alzheimer's disease, J. Alzheimers Dis. 65 (2018) 1445-1458. https://doi.org/10.3233/JAD-180623.

[32] P. Kundu, H.U. Lee, I. Garcia-Perez, et al., Neurogenesis and prolongevity signaling in young germ-free mice transplanted with the gut microbiota of old mice, Sci. Transl. Med. 11 (2019) eaau4760. https://doi.org/10.1126/scitranslmed.aau4760.

[33] J. Le Douce, M. Maugard, J. Veran, et al., Impairment of glycolysis-derived *L*-serine production in astrocytes contributes to cognitive deficits in Alzheimer's disease, Cell Metab. 31 (2020) 503-517.e8. https://doi.org/10.1016/j.cmet.2020.02.004.

[34] H.G. Lee, M.A. Wheeler, F.J. Quintana, Function and therapeutic value of astrocytes in neurological diseases, Nat. Rev. Drug Discov. 21 (2022) 339-358. https://doi.org/10.1038/s41573-022-00390-x.

[35] M.V. Sofroniew, H.V. Vinters, Astrocytes: biology and pathology, Acta Neuropathol. 119 (2010) 7-35. https://doi.org/10.1007/s00401-009-0619-8.

[36] J.V. Andersen, A. Schousboe, A. Verkhratsky, Astrocyte energy and neurotransmitter metabolism in Alzheimer's disease: integration of the glutamate/GABA-glutamine cycle, Prog. Neurobiol. 217 (2022) 102331. https://doi.org/10.1016/j.pneurobio.2022.102331.

[37] G. Bonvento, J.P. Bolanos, Astrocyte-neuron metabolic cooperation shapes brain activity, Cell Metab. 33 (2021) 1546-1564. https://doi.org/10.1016/j.cmet.2021.07.006.

[38] S. Takahashi, Neuroprotective function of high glycolytic activity in astrocytes: common roles in stroke and neurodegenerative diseases, Int. J. Mol. Sci. 22 (2021) 6568. https://doi.org/10.3390/ijms22126568.

[39] M. Bélanger, I. Allaman, P.J. Magistretti, Brain energy metabolism: focus on astrocyte-neuron metabolic cooperation, Cell Metab. 14 (2011) 724-738. https://doi.org/10.1016/j.cmet.2011.08.016.

[40] F.D. de Paula, D.S.L. Estessi, F. Duran, et al., Cannabidiol treatment improves glucose metabolism and memory in streptozotocin-induced Alzheimer's disease rat model: a proof-of-concept study, Int. J. Mol. Sci. 23 (2022) 1076. https://doi.org/10.3390/ijms23031076.

[41] S. Mason, Lactate shuttles in neuroenergetics-homeostasis, allostasis and beyond, Front. Neurosci. 11 (2017) 43. https://doi.org/10.3389/fnins.2017.00043.

[42] S. Sahar, V. Nin, M.T. Barbosa, et al., Altered behavioral and metabolic circadian rhythms in mice with disrupted NAD^+ oscillation, Aging 3 (2011) 794-802. https://doi.org/10.18632/aging.100368.

[43] L. Tian, Y. Tan, G. Chen, et al., Metabolism of anthocyanins and consequent effects on the gut microbiota, Crit. Rev. Food Sci. Nutr. 59 (2019) 982-991. https://doi.org/10.1080/10408398.2018.1533517.

[44] L. Lavefve, L.R. Howard, F. Carbonero, Berry polyphenols metabolism and impact on human gut microbiota and health, Food Funct. 11 (2020) 45-65. https://doi.org/10.1039/C9FO01634A.

[45] A. Bouyahya, N.E. Omari, N. El Hachlafi, et al., Chemical compounds of berry-derived polyphenols and their effects on gut microbiota, inflammation, and cancer, Molecules 27 (2022) 3286. https://doi.org/10.3390/molecules27103286.

[46] P. Liu, W. Zhou, W. Xu, et al., The main anthocyanin monomer from *Lycium ruthenicum* Murray fruit mediates obesity via modulating the gut microbiota and improving the intestinal barrier, Foods 11 (2022) 98. https://doi.org/10.3390/foods11010098.

[47] B. Tian, P. Huang, Y. Pan, et al., Tea polyphenols reduced obesity by modulating gut microbiota-SCFAs-barrier and inflammation in high-fat diet-induced mice, Mol. Nutr. Food Res. 68(24) (2024) e2400685. https://doi.org/10.1002/mnfr.202400685.

[48] B. Tian, Y. Geng, P. Wang, et al., Ferulic acid improves intestinal barrier function through altering gut microbiota composition in high-fat diet-induced mice, Eur. J. Nutr. 61 (2022) 3767-3783. https://doi.org/10.1007/s00394-022-02927-7.

[49] S. Zhao, A. Torres, R.A. Henry, et al., ATP-citrate lyase controls a glucose-to-acetate metabolic switch, Cell Rep. 17 (2016) 1037-1052. https://doi.org/10.1016/j.celrep.2016.09.069.

[50] G. Mithieux, The gut microbiota: stable bioreactor of variable composition?, Trends Endocrinol. Metab. 33 (2022) 443-446. https://doi.org/10.1016/j.tem.2022.04.005.

[51] G.F. Zhang, M.V. Jensen, S.M. Gray, et al., Reductive TCA cycle metabolism fuels glutamine- and glucose-stimulated insulin secretion, Cell Metab. 33 (2021) 804-817.e5. https://doi.org/10.1016/j.cmet.2020.11.020.

[52] M. Maugard, P.A. Vigneron, J.P. Bolanos, et al., *L*-Serine links metabolism with neurotransmission, Prog. Neurobiol. 197 (2021) 101896. https://doi.org/10.1016/j.pneurobio.2020.101896.

[53] Y. An, V.R. Varma, S. Varma, et al., Evidence for brain glucose dysregulation in Alzheimer's disease, Alzheimers Dement. 14 (2018) 318-329. https://doi.org/10.1016/j.jalz.2017.09.011.

[54] M. Fakhoury, Microglia and astrocytes in Alzheimer's disease: implications for therapy, Curr. Neuropharmacol. 16 (2018) 508-518. https://doi.org/10.2174/1570159X15666170720095240.

[55] H. Phatnani, T. Maniatis, Astrocytes in neurodegenerative disease, Cold Spring Harb. Perspect. Biol. 7(6) (2015) a020628. https://doi.org/10.1101/cshperspect.a020628.

[56] Z. Yang, K.K. Wang, Glial fibrillary acidic protein: from intermediate filament assembly and gliosis to neurobiomarker, Trends Neurosci. 38 (2015) 364-374. https://doi.org/10.1016/j.tins.2015.04.003.

[57] J. Ma, B.R. Choi, C. Chung, et al., Chronic brain inflammation causes a reduction in GluN2A and GluN2B subunits of NMDA receptors and an increase in the phosphorylation of mitogen-activated protein kinases in the hippocampus, Mol. Brain 7 (2014) 33. https://doi.org/10.1186/1756-6606-7-33.

[58] W. Koh, H. Kwak, E. Cheong, et al., GABA tone regulation and its cognitive functions in the brain, Nat. Rev. Neurosci. 24 (2023) 523-539. https://doi.org/10.1038/s41583-023-00724-7.

[59] G.A. Czapski, J.B. Strosznajder, Glutamate and GABA in microglia-neuron cross-talk in Alzheimer's disease, Int. J. Mol. Sci. 22(21) (2021) 11677. https://doi.org/10.3390/ijms222111677.

[60] J. Jiang, C. Sheng, G. Chen, et al., Glucose metabolism patterns: a potential index to characterize brain ageing and predict high conversion risk into cognitive impairment, GeroScience 44 (2022) 2319-2336. https://doi.org/10.1007/s11357-022-00588-2.